Anti-Cancer Drugs 1997, 8, pp. 245–256

In vitro cytotoxicity and DNA damage production in Chinese hamster ovary cells and topoisomerase II inhibition by 2-[2′-(dimethylamino)ethyl]-1,2-dihydro-3H-dibenz[*de,h*]isoquinoline-1,3-diones with substitutions at the 6 and 7 positions (azonafides)

Craig A Mayr,[1,3] Salah M Sami[2] and Robert T Dorr[3]
[1]Department of Pharmacology/Toxicology, [2]Department of Pharmaceutical Sciences and [3]Arizona Cancer Center, University of Arizona, Tucson, AZ 85724, USA.

The mechanism of action of a group of anthracene-containing analogs of amonafide was studied in Chinese hamster ovary (CHO) cells. These agents differ structurally from amonafide by the replacement of the naphthalene chromophore with an anthracene chromophore, the lack of a primary amine moiety in the 5 position, and substitutions at the 6 and 7 positions on the anthracene nucleus. In this study, five analogs with potent growth inhibitory activity and with low cardiotoxicity were chosen. Cytotoxicity analyses with tetrazolium dye assays (MTT) *in vitro* and continuous drug exposure revealed IC_{50} values in CHO cells in the nanomolar range. Intracellular scanning laser confocal microscopy of these drug-treated CHO cells showed that all analogs are able to enter cell nuclei with varying nuclear/cytoplasmic distribution: the more potent dimethylaminoethyl substituted analogs, 47 and 104, were primarily localized in the nucleus. Three analogs, including the unsubstituted parent (1), and numbers 35 (6-amino substituted) and 53 (6-aminoethyl substituted) inhibited DNA and RNA synthesis when assayed immediately after a 1 h exposure. In contrast, analogs 47 and 104 required 24 h post-drug exposure for 1 h to inhibit DNA and RNA synthesis. Using alkaline elution techniques, each analog also produced DNA single- and double-stranded breaks, as well as DNA–protein cross-links. Interestingly, the most cytotoxic analogs, 47 and 104, produced minimal DNA strand damage in CHO cells at their IC_{90} concentrations, whereas the three other compounds with lower growth inhibitory potency produced marked and roughly equivalent DNA damage at equitoxic concentrations. Gel shift analysis of SV40 DNA exposed to the compounds demonstrated that these agents do not directly induce DNA strand breaks. However, catalytic studies with purified human topoisomerase II (Topo II) and plasmid DNA demonstrated that these drugs inhibit this enzyme. These results suggest that the azonafides inhibit Topo II to cause protein-associated strand breaks and impaired DNA and RNA synthesis. However, other mechanisms may also be operant, especially with the more potent dimethylamino ethyl substituted analogs.

Key words: Alkaline elution, anthracene, azonafide, intercalation, strand breaks.

Introduction

The azonafide series of anthracene antitumor agents was derived from prior work by Braña *et al.* on a group of agents with a benzisoquinolinedione-type structure.[1] The newer azonafide compounds thus have a structural resemblance to amonafide,[1,2] but possess an anthracene chromophore rather than the naphthalene chromophore found in amonafide. Amonafide was shown to inhibit cancer cell growth *in vitro*, and in early clinical trials a few responses were reported in hormone refractory prostate cancer[3] and metastatic breast cancer.[4] Neutropenia is dose limiting for this agent.[5] The parent compound in the new series is the unsubstituted anthracene designated as analog number **1** or azonafide. It has shown significant enhancement of antitumor potency over amonafide when tested against a panel of human and murine tumor cells *in vitro*, and it has a reduced *in vitro* cardiotoxicity in rat cells compared to cytotoxic potency in tumor cell lines relative to that of amonafide.[6,7] Many

This article was supported by grant GM 49875 from the National Institute of Health and National Cancer Institute. Its contents are solely the responsibility of the authors and do not necessarily represent the official views of the National Cancer Institute.

Correspondence to RT Dorr, Arizona Cancer Center, PO Box 245024, 1515 N Campbell Avenue, Tucson, AZ 85724, USA. Tel: (+1) 520 626-7892; Fax: (+1) 520 626-2284

© 1997 *Rapid Science Publishers*

derivatives of azonafide have been synthesized and tested in a bank of human and murine tumor cell lines and in the neonatal rat heart myocyte cardiotoxicity assay.[8] These analogs include compounds with various substitutions at the 6 and 7 position of the anthracene nucleus. Prior mechanistic investigations with some of these analogs have shown that antitumor cytotoxic potency is roughly proportional to DNA intercalation, noted by increased stability against thermal denaturation of double-stranded calf thymus DNA.[7] Similarly, mechanistic studies with amonafide showed dose-related DNA single-strand breaks (SSB) and DNA–protein cross-links (DPC) characteristic of topoisomerase II (Topo II) inhibition.[9]

The current study was designed to characterize the mechanism of action of a select group of azonafide analogs. Specific analogs were chosen for study based on their performance in the cytotoxicity studies. Four analogs were selected from the 160 that have been synthesized due to their high cytotoxic potency in four human tumor cell lines along with a relatively low toxic potency in the fetal rat heart myocyte cardiotoxicity model.[10] Figure 1 shows the unsubstituted analog (azonafide, **1**) and lists the substitutions on the four azonafide analogs, numbered **35**, **47**, **53** and **104**. In the current study, these five compounds were tested for their growth inhibitory potency, intracellular distribution, and their ability to inhibit macromolecular synthesis and produce DNA damage all in Chinese hamster ovary (CHO) cells. Further analysis was done to determine if these compounds could directly damage DNA. Finally, these drugs were tested for the ability to inhibit Topo II in a cell-free system using purified human Topo II enzyme and plasmid DNA.

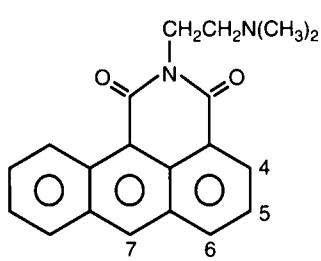

Analog number	Substitution
1	none
35	7-NH_2
47	6-$NH(CH_2)_2N(CH_3)_2$
53	6-OCH_2CH_3
104	6-$O(CH_2)_2N(CH_3)_2$

Figure 1. Structures of azonafides used in the study.

Methods

Drugs

Azonafide analogs were synthesized in the laboratory of William Remers and purified by chromatography. The structures were confirmed using NMR and compositional analytical techniques as previously described.[6,7] They were reconstituted into stock solutions of 2 mg/ml (or 1 mg/ml for analog **53**) in dimethyl sulfoxide (DMSO) (JT Baker, analytical grade) and kept at −20°C. Previous studies in this laboratory have shown these drugs to be stable when stored in this manner (unpublished data).

Cell culture

Chinese hamster ovary cells (ATCC CCL 61) were obtained from American Type Culture Collection (Rockville, MD). Cells were maintained in PDRG basal media (HyClone, Logan, UT) supplemented with 2 mM L-glutamine, 100 units/ml penicillin and 100 μg/ml streptomycin (Irvine Scientific, Santa Ana, CA), and 5% iron-enriched calf serum (Intergen, Purchase, NY). Cells were incubated at 37°C in air with 100% relative humidity. Cells were tested bimonthly and confirmed to be mycoplasma-free using a mycoplasma ELISA detection kit (Boehringer Mannheim, Indianapolis, IN).

Microculture tetrazolium assay

This assay is based on reductive cleavage of 3-(4,5-dimethylthiazol-2-yl)-2,5-diphenyl-2H-tetrazolium (MTT) bromide to a colored formazan compound as an indicator of cell viability.[10] CHO cells were plated at 1000/well onto 96-well microtiter plates (Costar, Cambridge, MA). On day 2, drugs dissolved initially in DMSO and then diluted serially with phosphate buffered saline (PBS) (pH 7.4) were added at concentrations of 0.5 nM to 10 μM in half-log gradations. Final concentrations of DMSO did not exceed 0.1%. Drugs were either removed after 1 h of incubation or were left on the plates for a 5 day exposure. The plates were incubated at 37°C in air with 100% relative humidity for 5 days.

After the 5 day incubation period, 50 μl of a 1 mg/ml MTT solution was added to each of the wells and the plates were incubated an additional 4 h. The medium was then aspirated and the formazan product was solubilized by DMSO (100 μl/well). The intensity of the color, which is proportional to viable

cell numbers, was quantified by absorbance at 570 nm on an automated microculture plate reader (Biomek 1000; Beckman Instruments, Fullerton, CA). Test results were calibrated in percent control absorbance from untreated CHO cells. Each drug concentration was tested in three to six independent experiments, and the IC_{50} and IC_{90} values were determined by regression analysis of the linear portion of the dose–response curve for each analog.

Scanning laser confocal microscopy (SLCM)

Intracellular drug distribution was studied by examining drug-treated cells under SLCM, as these drugs are autofluorescent due to their anthracene nucleus. Briefly, 1×10^6 cells were seeded onto sterilized glass coverslips and allowed to attach overnight. The cell coated coverslips were then exposed to the 1 h IC_{90} of each analog for 1 h at 37°C. After incubation, coverslips were washed three times with PBS. Cells were then fixed with 4% neutral buffered formalin for 10 min, followed by two additional washes with PBS (5 min each). The coverslips were then mounted onto glass microscope slides with fluorescent mounting medium (DAKO, Carpinteria, CA). Slides were then observed and imaged using a Leica TCS-4D scanning laser microscope (Heidelberg, Germany) equipped with a 100× oil immersion lens (1.4 numerical aperture), an epi-fluorescent xenon lamp and a fluorescein-5-isothiocyanate (FITC) filter.

Macromolecular synthesis inhibition assay

The inhibition of DNA, RNA and protein synthesis was investigated using a modification of the nuclide incorporation method of Li *et al.*[11] Sterilized, chromic acid-washed glass scintillation vials (Research Products International, Mount Prospect, IL) were seeded with 500 000 cells in 2.0 ml media. Vials were incubated at 37°C overnight. Following incubation, the incubation media was discarded and 1.0 ml warmed fresh media containing the 1 h IC_{90} of the desired analog was pipetted into each vial. The vials were then placed back into the incubator for 2 h. During the last hour of exposure, 1 μCi [^{3}H]thymidine, [^{3}H]uridine or [^{14}C]valine (ICN Radiochemicals, Irvine, CA) for the measurement of DNA, RNA or protein synthesis, respectively, was added to the appropriate vials either immediately or 24 h following exposure. After 1 h the media was removed. Vials were then rinsed three times with cold PBS (pH 7.4) and three times with cold 5% trichloroacetic acid (TCA). The TCA rinses were saved to determine the amount of unincorporated precursor in the cytosol. Following the final TCA wash, a final 0.5 ml 5% TCA was added and the vials were incubated in an oven at 80°C for 30 min. Upon cooling, 15 ml of acidified Eco-Lite scintillation cocktail (ICN) was added to each vial. Vials were counted in a Beckman model LS 3801 scintillation counter and percentages of control of [^{3}H]thymidine, [^{3}H]uridine or [^{14}C]valine c.p.m. were calculated. The following positive controls were used, aphidicolin (2 μg/ml) to inhibit DNA synthesis (13), actinomycin D (1 μg/ml) to inhibit RNA synthesis (14) and cycloheximide (5 μg/ml) to inhibit protein synthesis.[14] Data were analyzed for statistical significance using Student's *t*-test for grouped data.

Alkaline DNA elution for detection of DNA SSB, DPC and DNA double-strand breaks (DSB)

The technical and theoretical aspects of this procedure have been reviewed in detail elsewhere.[15] Briefly, CHO cells were seeded at 500 000 cells/25 cm^2 flask and labeled with 140 nCi [^{14}C]thymidine for 3 days prior to the experiment. Cells were then exposed to the 1 h IC_{90} of each analog for 1 h, removed and then washed by centrifugation in cold medium. One million cells (500 000 cells for DSB determinations) were then loaded gently into 50 ml filter stacks housing a 25 mm, 2 μm pore size polyvinylchloride filter (Type BS; Millipore, San Francisco, CA) for SSB and DPC tests, or a polycarbonate capillary pore filter (Nucleopore, Pleasanton, CA) for DSB determinations. The cells were washed with ice cold PBS and lysed immediately on the filters with 3 ml of 0.07 M SDS, 7.5 mg/ml glycine, 0.02 M Na_2EDTA (pH 10.0) for SSB determinations, 2.0 M NaCl, 0.04 M Na_2EDTA, 0.2% *N*-lauryl-sarcosine (pH 10.0) for DPC determinations, or 0.05 M Tris, 0.05 M glycine, 0.25 M Na_2EDTA, 2% w/w SDS, 0.5 mg/ml freshly reconstituted proteinase K (FisherBiotech, Fair Lawn, NJ; from *Tritirachium album*, activity about 30 U/mg protein). For SSB assays, unirradiated cells were lysed and the lysate was treated for 1 h with lysis solution containing 0.5 mg/ml proteinase K. DNA was then eluted with a solution of 0.035 M SDS, 0.02 M EDTA (free acid) and 25% tetrapropylammonium hydroxide (TPAH) adjusted to pH 12.1 with TPAH. A positive control of cells irradiated to 6.5 Gy (X-ray) was included in

each experiment. To assess whether DPC were produced by the analogs, following drug exposure, cells were irradiated to a total of 30 Gy (X-ray) to produce very short DNA strands which are retained on the filter only if the DNA strand is covalently linked to a large protein.[16] DNA was then eluted with a solution of 0.02 M Na_2EDTA adjusted to pH 12.1 with TPAH. For DSB determinations, cells were lysed for 1 h. DNA was then eluted with the same solution used in the lysing step (proteinase K free). A positive control of cells irradiated to 100 Gy (X-ray) was included in each experiment.

Prior to the elution step in the SSB and DPC assays, all filters were rinsed twice with 0.02 M Na_2EDTA adjusted to pH 10.0 with TPAH. All cell lysis and DNA elution steps were performed in the dark to prevent UV light-induced DNA damage.[17] Elution was performed by peristaltic pumping (Rabbit peristaltic pump; Ranin, Woburn, MA) of the elution solution through the filters at a rate of approximately 2.5 ml/h for 13–15 h. Fractions of 2.5–3.0 ml were collected at 60 min intervals. Radioactivity (^{14}C c.p.m.) in the elution fractions and filters was determined by scintillation counting after dilution into 15 ml of acidified scintillation fluid (0.5% acetic acid). The total amount of radioactive DNA was collected from each experiment to facilitate quantitation of SSB, DPC and DSB without the use of an internal standard, such as ^3H-counter-labeled DNA control cells.[18] A standard curve of slope in SSB experiments versus dose of radiation was generated for CHO cells and the slope of each drug treated curve was used to determine the Gy equivalents for the SSB production. The DPC lesions were converted to Gy-equivalents (*Pc*) using the bound-to-one-terminus model of Ross *et al.*:[19]

$$Pc = [(1 - r)^{-1} - (1 - r_0)^{-1}]^{Pb}$$

where *Pb* is the frequency of DNA SSB produced by 30 Gy, and r and r_0 are the fractions of DNA eluting in the slow elution phase in the presence or absence of drug, respectively. The degree to which r exceeds r_0 is a measure of DPC.

Direct DNA damage assay

Direct drug-induced DNA damage was measured by band shift analysis of supercoiled SV40 plasmid DNA after incubation with each of the analogs and agarose gel electrophoresis. Assays were performed in a total volume of 25 μl which contained 0.5 μg SV40 plasmid DNA (Gibco/BRL, Grand Island, NY) and 10 μM desired analog in a reaction buffer containing 0.01 M Tris–HCl, 0.05 M KCl, 0.05 M NaCl, 0.005 M $MgCl_2$ and 0.0001 M Na_2EDTA (pH 7.4). Samples were incubated at 37°C for 60 min. After incubation, 10 μl of 5 M NaCl was added and the drugs were extracted three times with 100 μl hydrated *n*-butanol. After drug extraction the DNA was ethanol precipitated (−20°C, 1 h) and was reconstituted in 10 μl reaction buffer to which was added 1 μl of a loading buffer consisting of 40% (w/v) sucrose and 0.25% bromophenol blue. The DNA samples were run on a 1% agarose gel with a running buffer of 0.045 M Tris–borate and 0.001 M Na_2EDTA. The gel was run at 120 V for 2 h, stained for 30 min with ethidium bromide (EtBr) (2 μg/ml) and destained in 0.002 M $MgCl_2$ before photographing. Positive controls included incubations with 0.3 U Topo I and 5.0 U *Eco*RI (both from Gibco/BRL) to produce the relaxed circular and linearized plasmids, respectively.

Topo II inhibition assay

Drug-induced Topo II inhibition was assessed using the Topoisomerase II Drug Screening Kit from TopoGEN (Columbus, OH). Briefly, 0.5 μg pRYG plasmid, which contains a single high-affinity Topo II cleavage and recognition site, was incubated with increasing concentrations of each analog plus purified human Topo II (6 U). Incubations were carried out at 37°C for 30 min in cleavage buffer (30 mM Tris–HCl, pH 7.6, 3.0 mM ATP, 15 mM mercaptoethanol, 8.0 mM $MgCl_2$, 60 mM NaCl). The reaction was stopped and cleavable complex trapping was accomplished by the addition of 1/10 volume of 10% SDS. Proteinase K was then added (50 μg/ml) and the samples were incubated at 37°C for an additional 30 min. One-tenth volume of loading dye (0.25% bromophenol blue, 50% glycerol) was added and samples were extracted twice with chloroform:isoamyl alcohol (1:24). Samples were electrophoresed on a 1% agarose gel containing 0.5 μg/ml EtBr at 45 V overnight in 4 × TAE buffer (20) also containing 0.5 μg/ml EtBr. Gels were destained for 30 min in H_2O and photographed (Fotodyne system, Polaroid® 667 film, 0.5 s/*f*5.6).

Results

The survival of CHO cells following 1 h and 5 day exposure to various concentrations of the azonafide analogs as determined by the microculture tetrazolium assays revealed IC_{90}s that ranged from approxi-

mately 10 to 1000 nM and from 3 to 60 nM in the 1 h and 5 day exposure experiments, respectively (Table 1). The order of potency of the analogs was not conserved between the 1 h and 5 day exposure time experiments, although analog numbers **47** and **104** were consistently most potent in both time courses. They were followed (in descending potency) by numbers **53**, **1** and **35** for the 1 h incubation, and **35**, **53** and **1** for the 5 day exposure. However, the order of potency was conserved between the IC_{50} and IC_{90} values, within each incubation time (data not shown).

Table 1. Activity of azonafide analogs in MTT cytotoxicity assays with CHO cells

Exposure time[a]	Analog	IC_{90} [nM (ng/ml)]
1 hour	**1**	627 (221.3)
	35	1030 (380.1)
	47	11.3 (5.4)
	53	431 (171.1)
	104	31.5 (15.1)
5 day	**1**	61.8 (21.8)
	35	35.4 (13.1)
	47	3.13 (1.5)
	53	41.4 (16.4)
	104	3.94 (1.9)

[a]Continuous drug exposure time in the MTT assay, total incubation time in all assays was 5 days.

Intracellular drug distribution was studied by examining CHO cells treated with the 1 h IC_{90} concentration of each individual analog using SLCM. All the drugs were visualized in the nuclei of CHO cells, but there were distinctly different specific patterns of nuclear–cytoplasmic distribution. The two most potent cytotoxic analogs, **47** and **104**, localized almost exclusively in the nuclei, with little or no staining found in the cytoplasm (Figure 2d and f). Analogs **1** and **35** were localized primarily in the nuclei, but diffuse cytoplasmic staining was also observed (Figure 2b and c). In contrast, analog **53** was found primarly in the cytoplasm in a vesicular type of distribution, with much less staining seen in the nuclei of the CHO cells (Figure 2e).

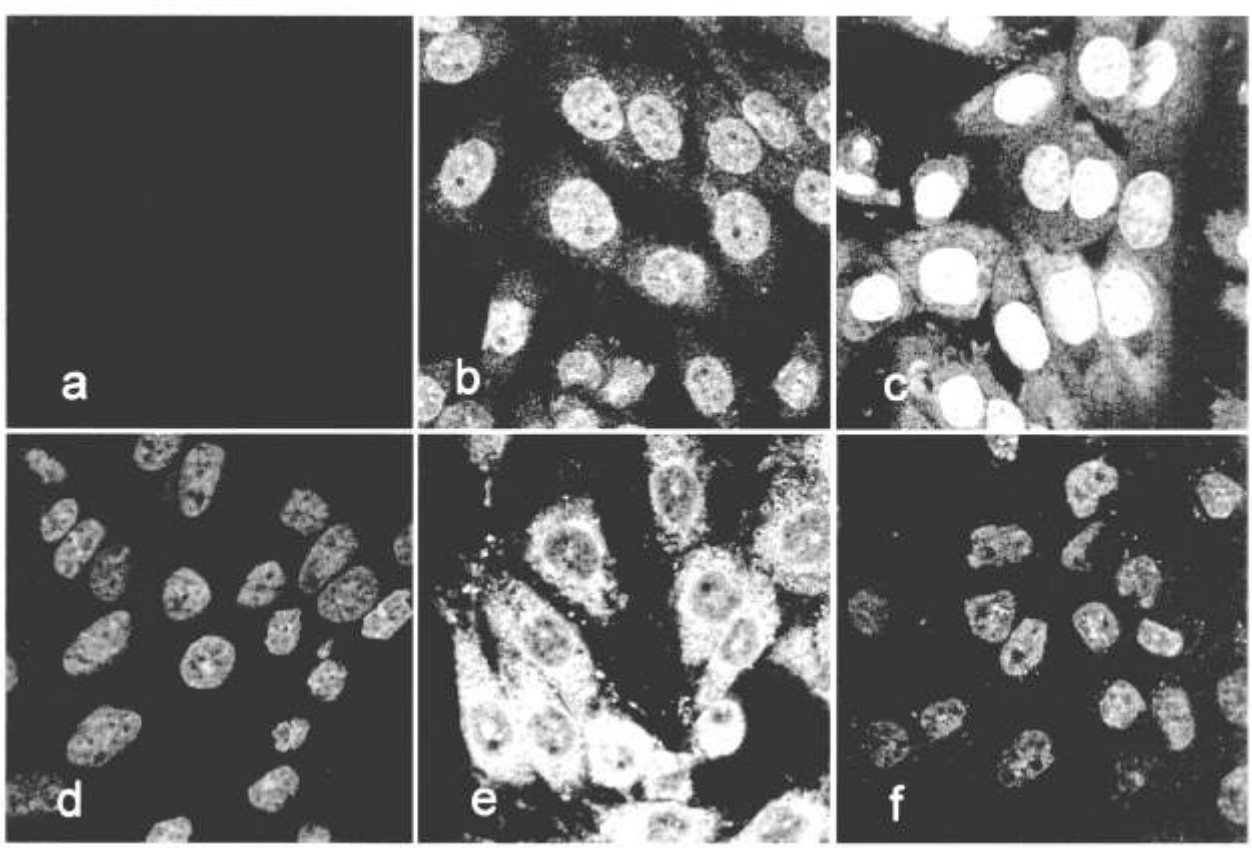

Figure 2. Intracellular distribution of analogs in CHO cells. Glass coverslips coated with CHO cells were incubated with the IC_{90} of each analog for 60 min at 37°C, fixed with 4% NBF and imaged using a scanning laser confocal microscope (Leica TCS-4D, 100X-1.4a, using a FITC filter). (a) Undrugged control, (b) **1**, (c) **35**, (d) **47**, (e) **53** and (f) **104**.

The ability of these drugs to inhibit macromolecular synthesis was investigated using a radionuclide incorporation assay. Figure 3(a and b) shows that analogs **53**, **1** and **35**, when tested at the 1 h IC_{90} concentrations, were capable of inhibiting DNA and RNA synthesis to biologically significant levels. Analogs **1**, **35** and **53** each inhibited DNA and RNA synthesis to approximately 50% of that seen for untreated controls. An exception was analog **53**, which was slightly more inhibitory toward RNA synthesis (to approximately 65% of control). However, at 24 h after the 1 h exposure, all five analogs inhibited DNA and RNA synthesis to less than 20 and 50% of control values, respectively. TCA extracts of the samples showed that drug-exposed samples contained equal or higher levels of unincorporated precursor compared to the untreated control samples at both the 1 and 24 h time points (data not shown). This shows that nucleotide-precursor uptake was not inhibited by the azonafides. Protein synthesis was also not inhibited by any of the analogs at either time point (Figure 3c).

The ability of these drugs to produce DNA damage in CHO cells was assessed by alkaline elution techniques. Figure 4(a) displays the results from the assessment of SSB production by the analogs. These results represent the strand breaking ability of the drugs normalized to cell killing at the same 1 h IC_{90} concentrations defined earlier. The data from these experiments are used to generate a curve showing the percent [^{14}C]DNA remaining on the filter versus elution time for each analog. A drug's ability to produce SSBs is revealed by an increase in the slope of this curve relative to untreated controls. The greater slope indicates a higher frequency of SSB production with resultant smaller sized DNA fragments. As shown in the top curve of Figure 4(a), the slope for untreated cells (which is assumed to have 100% of the [^{14}C]DNA retained on the filter) is at 0.4, and for the 6.5 Gy irradiated positive control, 8.9. The other curves demonstrate that all five compounds produced SSB in the CHO cells, with varying efficiency. Analogs **47** and **104**, the most potent cytotoxic agents in the study, showed low efficiency in producing SSB in the CHO cells with only a slightly larger slope than untreated control (4.1 and 4.6, respectively). This indicates a relatively small amount of DNA SSB; with most of the intact DNA strands in these samples being trapped on the filter during the elution. Conversely, the other three

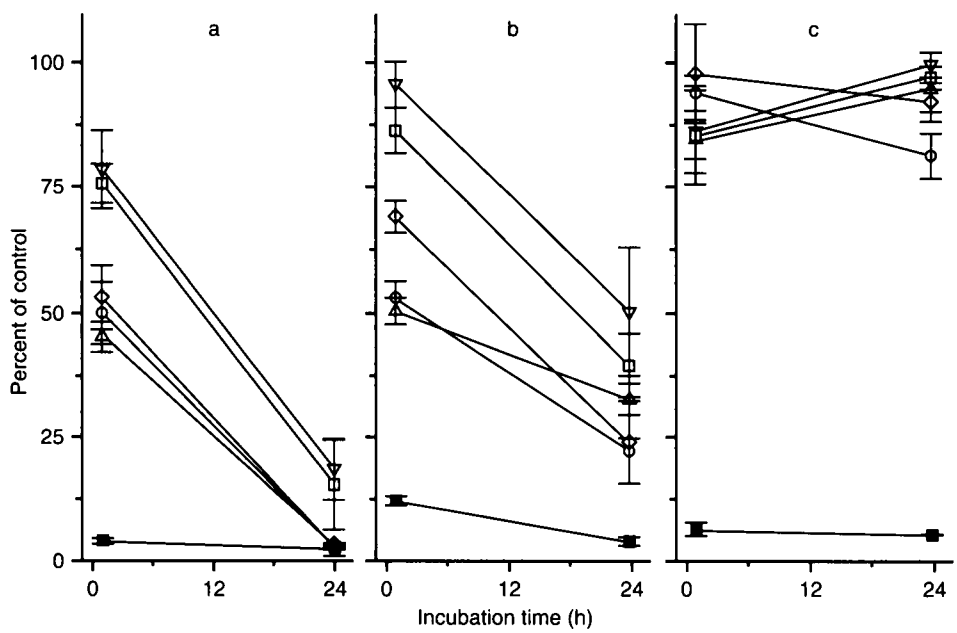

Figure 3. Inhibition of macromolecular synthesis in CHO cells by analogs of azonafide. Cells were treated with the IC_{90} of each analog for 1 h, at which point radiolabeled precursor molecules were added for an additional hour either immediately or 24 h later. Symbols represent mean values ± SEM of three independent experiments expressed as percent of untreated control values. Positive control consisted of aphidicolin for DNA synthesis, actinomycin D for RNA synthesis and cycloheximide for protein synthesis. Panel (a) represents DNA synthesis, panel (b) represents RNA synthesis and panel (c) represents protein synthesis. In each panel, closed squares represent relevant positive controls, open circles represent **1**, open upward triangles represent **35**, open downward triangles represent **47**, open diamonds represent **53** and open squares represent **104**.

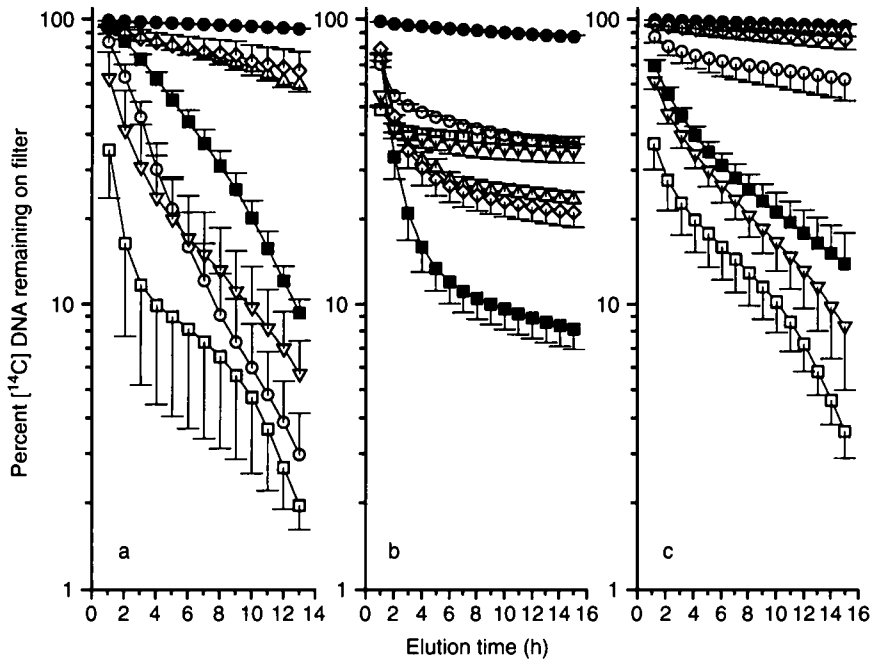

Figure 4. DNA SSB (a), DPC (b) and DNA DSB (c) by azonafide analogs in CHO cells. Cells were treated with the IC_{90} of each analog for 60 min at 37°C. DNA SSB, DPC and DSB were quantified by filter elution and expressed as percent [^{14}C]DNA remaining on filters. Points are means ± SEM of three independent determinations (four to seven independent experiments for the DSB determinations). In each panel closed circles represent control, closed squares represent X-ray control, open squares represent **1**, open circles represent **35**, open upward triangles represent **47**, open downward triangles represent **53** and open diamonds represent **104**.

analogs, **1**, **35** and **53**, produced a higher frequency of SSBs, demonstrated by the relatively large increase in their slopes (29.4, 18.0 and 23.1, respectively) compared to the untreated control. The results in Figure 4 further show that these three analogs were approximately equivalent in their ability to produce SSBs. Table 1 lists the Gy equivalents calculated for each analog's ability to produce DNA SSB. This shows that analogs **1**, **35** and **53** produced SSB approximately equivalent to 2.3, 4.5 and 3.3 Gy of X-ray damage, respectively. In contrast, analogs **47** and **104** produced SSBs equivalent to only 1.5 and 0.9 Gy of X-ray damage, respectively.

Additional alkaline elution experiments compared the analogs' ability to produce DPC in the CHO cells (Figure 4b). Again, the 1 h IC_{90} for each analog was used in these experiments to normalize the results for growth inhibitory potency. In these experiments, cells are exposed to drugs for 1 h, after which all samples except the non-irradiated, untreated controls are irradiated to 30 Gy to produce very small DNA fragments. These DNA fragments will elute very rapidly, unless they are covalently linked to large proteins, in which case they will be retained on the filter. Similar to what was seen in the SSB assay, the analogs each produced DPC with varying efficiency. Figure 4(b) shows that the DNA from cells treated with analogs **47** and **104** was not retained on the filter to the same extent as was the DNA from the samples treated with compounds **1**, **35** and **53**. This indicates that analogs **1**, **35** and **53** produced more DPC. These results show that the pattern of effectiveness of these compounds to produce DPC is roughly the same as that for the production of SSB. Specifically, the highly potent analogs **47** and **104** were less efficient than the less potent compounds **1**, **35** and **53** at producing DPC. Gray equivalents were also determined for the number of DPC formed after exposure to the 1 h IC_{90}s of these drugs. The results are listed in Table 2. The results of these analyses indicate that analogs **1**, **35** and **53** produced DPC equivalent to that of cells exposed to 15.6, 27.2 and 14.7 Gy, respectively. Analogs **47** and **104** both produced DPC equivalent to that of an exposure to approximately 8 Gy.

Filter elution techniques were also used to determine if the analogs could produce DSB in CHO cells. The results of the experiments are shown in Figure 4(c). Again, cells were exposed to the 1 h IC_{90} of each analog for 1 h at 37°C immediately prior to

Table 2. Gy equivalents of azonafide analogs producing SSB and DPC in CHO cells[a]

Analog	SSB Gy equivalent	DPC Gy equivalent (r)
1	2.3	15.6 (0.41)
35	4.5	27.2 (0.52)
47	1.5	7.6 (0.30)
53	3.3	14.7 (0.40)
104	0.9	8.2 (0.31)

[a]CHO Cells were exposed to the IC_{90}s of the compounds for 1 h. Gy equivalents were determined using the slope versus radiation dose standard curve for SSB and for DPC, the equation $Pc = [(1-r)^{1} - (1-r_0)^{1}]^{Pb}$ as detailed in Methods. For the DPC determinations, $Pb = 30$ Gy and $r_0 = 0.15$.

chilling for loading onto filters and eluting with the pH 10 buffer. Analogs **1** and **53** produced a high frequency of DSB relative to untreated controls. Analogs **47** and **104** produced no DSB demonstrated by their elution curves being the same as the untreated control curve. Analog **35** produced DSB at a frequency greater than analogs **47** and **104**, yet less than analogs **1** and **53**. Once again the pattern of the highly cytotoxic compounds producing relatively less DNA damage at equitoxic doses is maintained.

The ability of the drugs to directly damage DNA was further assessed using gel shift analysis. In these experiments, negatively supercoiled SV40 plasmid DNA was exposed to 10 μM of each analog for 1 h. This drug concentration represents a highly toxic dose to CHO cells. The drugs were then extracted from the DNA, which was run on an agarose gel for analysis of the banding pattern. The principle of this assay is that if the drugs directly caused DNA strand scission, a band shift would occur proportional to the change in DNA size. If the drugs produced SSB in the SV40 plasmid, a relaxed circular plasmid would result. This relaxed circular plasmid would then migrate differently in the gel, producing a band shift. Topo I, which is known to produce a relaxed plasmid from a supercoiled plasmid,[9] was employed in these experiments as a positive control. Thus, if any of the analogs produced DSB, the result would be a linear plasmid. This would result in an altered migration of the DNA band through the gel in the case of a linearized plasmid. The restriction enzyme, *Eco*RI, which produces one DSB in the SV40 plasmid resulting in a linear plasmid, was used as a positive control in the experiments. If the DNA shearing was extensive enough, a fragmented plasmid would be produced, resulting in a laddering or smearing of the DNA band in the agarose gels.

Figure 5 displays a typical migration pattern obtained from these experiments. Lanes 1 and 2 are DNA size markers for supercoiled and linear DNA fragments, respectively. Lane 3 is untreated SV40 plasmid. Positive controls are shown in lanes 4 and 5; lane 4 is SV40 plasmid treated with 0.3 U Topo I (relaxed circular plasmid) and lane 5 is SV40 plasmid treated with 5.0 U *Eco*RI (linearized plasmid). The SV40 plasmid is a 5.2 kb circular DNA, and its linearized form, from *Eco*RI digestion, migrates very closely to the 5 kb fragment in the linear DNA size marker (lane 2). Lanes 6–10 are samples of SV40 plasmid incubated with analogs **1**, **35**, **47**, **53** and **104**, respectively (10 μM each). In all incubations

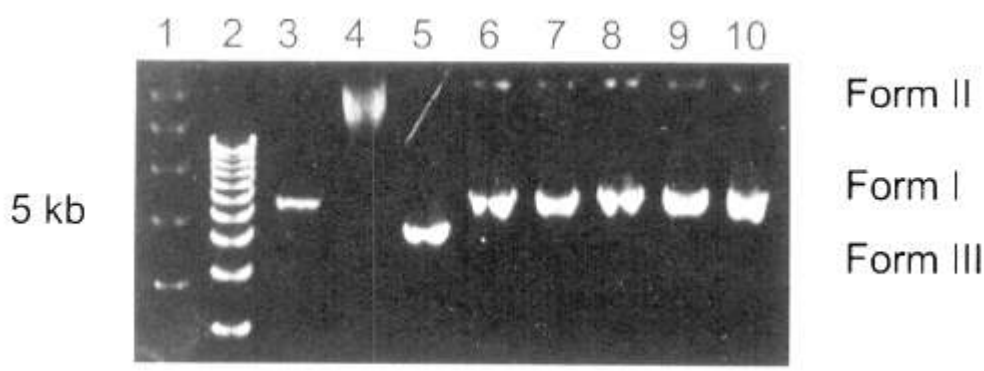

Figure 5. Direct DNA damage assessment for azonafide analogs. Each azonafide analog (10 μM) was incubated with closed, circular SV-40 DNA (0.5 μg) for 60 min at 37°C. Analogs tested were **1** (lane 6), **35** (lane 7), **47** (lane 8), **53** (lane 9) and **104** (lane 10). Control lanes were lanes 3, 4 and 5. SV40 DNA (form I) alone (lane 3). Topoisomerase incubated with the SV40 plasmid to produce a circular relaxed (form II) plasmid (lane 4). *Eco*RI-treated SV-40 to produce a linearized (form III) plasmid (lane 5). Size markers for supercoiled (lane 1) and linear DNA (lane 2) are included.

with the five azonafide analogs, no band shift was observed, indicating that these drugs do not directly cause SSB or DSB in supercoiled plasmid DNA.

Finally, these drugs were screened for the ability to inhibit purified Topo II using a commercial assay kit (TopoGEN). In this cell-free assay, 0.5 μg of negatively supercoiled pRYG plasmid DNA is incubated with increasing concentrations of drug plus purified human Topo II. The pRYG plasmid contains a high-affinity Topo II recognition site and thus makes an excellent substrate for Topo II activity and studies of Topo II inhibition. Figure 6 displays a typical migration pattern obtained by this assay. Lane 1 shows the banding pattern of the pRYG plasmid alone. The three distinct bands represent the supercoiled plasmid in its monomer, dimer and trimer concatemer forms where the monomer has the longest migration in the gel and the trimer has the shortest. Lane 2 contains only linear pRYG DNA (form III DNA). Lanes 3 and 4 contain the pRYG plasmid plus Topo II with or without DMSO, showing that the drugs' vehicle does not effect Topo II activity on the plasmid. A shift in the three bands relative to lane 1 are the result of catalytic activity of Topo II and represent the relaxation pRYG plasmid. Lanes 5 and 6 contain VP-16 (etoposide) at 0.05 and 0.5 mM, respectively. In lane 6, there is an increase in both form III and open circular (OC) DNA, resulting from the trapping of cleavable complexes of Topo II and DNA that were isolated upon addition of SDS. The DNA fragments were then freed from the Topo II by addition of proteinase K to the samples. Lanes 7–10 represent incubations of the plasmid and Topo II with mitoxantrone (MTX), a drug structurally similar to the azonafides. Lane 7 shows that the migration of pRYG DNA was not affected by incubation with MTX (10.0 μg/ml) alone. Lanes 8–10 show that when pRYG DNA was incubated with Topo II and 0.1, 1.0 and 10.0 μg/ml MTX, Topo II-mediated relaxation of pRYG DNA was inhibited in a dose-dependent manner. These lanes also show that there was no evidence of cleavable complex trapping in these samples. Lanes **11**, **15**, **19**, **23** and **27** show that migration of pRYG DNA was not affected by incubation alone with analogs **1**, **35**, **47**, **53** and **104**, respectively, at 5 μg/ml. Lanes 12–14, 16–18, 20–22, 24–26 and 28–30 all represent incubations of pRYG DNA with Topo II and analogs **1**, **35**, **47**, **53** and **104**, respectively. For each drug, Topo II-induced relaxation of pRYG DNA was

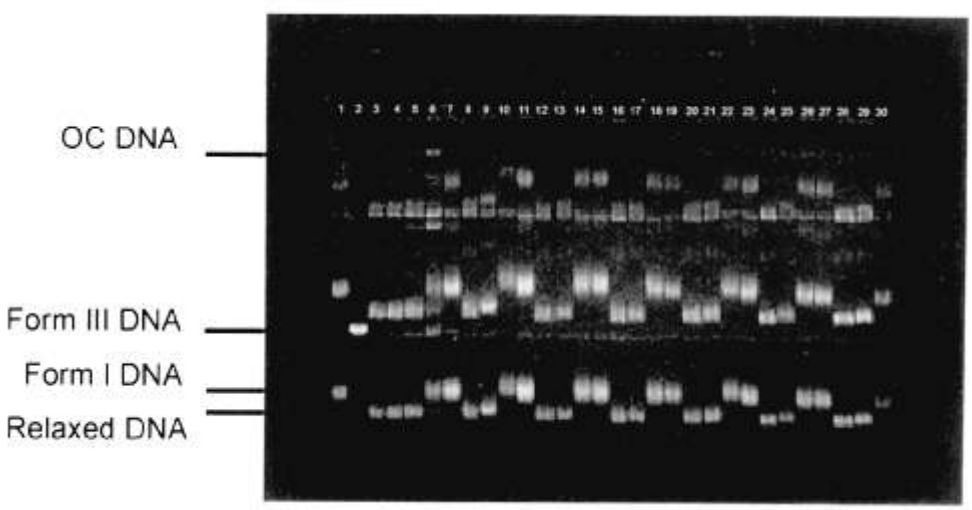

Figure 6. Inhibition of Topo II by azonafide analogs. Incubations of pRYG DNA, purified Topo II and analogs were performed in cleavage buffer for 30 min at 37°C followed by SDS addition and proteinase K digestion for 30 min at 37°C. Lane 1 is pRYG DNA alone, lane 2 is reference linear (form III) pRYG DNA, lanes 3 and 4 are pRYG DNA and Topo II with and without DMSO vehicle control, respectively, lanes 5 and 6 are pRYG plus Topo II plus VP-16 at 0.05 and 0.5 mM, respectively, lane 7 contains MTX (10 μg/ml) with pRYG alone, lanes 8–10 contain MTX (0.1, 1.0 and 10 μg/ml, respectively) with pRYG and Topo II, lane 11 contains **1** (5 μg/ml) with pRYG DNA alone, lanes 12–14 contain **1** (0.05, 0.5 and 5 μg/ml, respectively) with pRYG DNA and Topo II, lane 15 contains **35** (5 μg/ml) with pRYG DNA alone, lanes 16–18 contain **35** (0.05, 0.5 and 5 μg/ml, respectively)) with pRYG DNA and Topo II, lane 19 contains **47** (5 μg/ml) with pRYG DNA alone, lanes 20–22 contain **47** (0.05, 0.5 and 5 μg/ml, respectively) with pRYG DNA and Topo II, lane 23 contains **53** (5 μg/ml) with pRYG DNA alone, lanes 24–26 contain **53** (0.05, 0.5 and 5 μg/ml, respectively) with pRYG DNA and Topo II, lane 27 contains **104** (5 μg/ml) with pRYG DNA alone, and, finally, lanes 28–30 contain **104** (0.05, 0.5 and 5 μg/ml, respectively) with pRYG DNA and Topo II.

inhibited in a dose-dependent manner. Like MTX, there is no evidence of cleavable complex trapping by any of the analogs, noted by the absence of increased form III or OC DNA.

Discussion

The azonafide analogs were found to be highly cytotoxic to CHO cells *in vitro* (Table 1). The relatively small differences in IC_{90}s observed between the 1 h and 5 day drug exposure experiments suggest that these drugs act in a non-cell cycle-dependent manner, since the magnitudes of increases in cytotoxic potencies range from approximately 10- to 30-fold for the 1 h exposure compared to the 5 day (120 h) exposure times. Clearly, these differences are not the several log order increases expected for a brief versus a continuous exposure as is typically seen with a drug acting in a specific phase of the cell cycle.[21]

The analogs demonstrating the highest growth inhibitory potency were **47** and **104**. These two drugs have substitutions at the 6 position which are *N*- and *O*-linked (dimethylamino)ethyl groups. The (dimethylamino)ethyl side chain structure is also found on the isoquinoline-1,3-dione structure in all the analogs, in the 2 position. Analogs **47** and **104** are found to localize exclusively to the CHO cell nuclei, whereas analogs **1** and **35** primarily localize to the nuclei, but are also found in the cytoplasm. In contrast, analog **53** produced relatively low drug levels in the nuclei, with greater fluorescence noted in the cytoplasm, which appeared to be localized to unidentified vesicles (Figure 2e). This suggests that the side chains on analogs **47** and **104** help to localize the drugs in the nuclei of the CHO cells, which may explain the increased potency of these two analogs. Analogs **1**, **35** and **53** are found in the nucleus but are also distributed throughout the cytoplasm, and therefore higher drug levels may be required to achieve a critical nuclear concentration for interactions with the DNA.

In contrast, there was little evidence of nuclear damage for compounds **47** and **104**. In the macromolecular synthesis inhibition studies, analogs **47** and **104** showed little inhibition of DNA and RNA synthesis in CHO cells immediately after the 1 h IC_{90} exposure. The other three analogs all significantly inhibited DNA and RNA synthesis in the cells at this early time point. However, 24 h after the IC_{90} exposure, analogs **47** and **104** did significantly inhibit these processes and to about the same extent as did the other three agents (Figure 3a and b). Thus, despite rapid and selective nuclear localization of analogs **47** and **104**, the two drugs seem to have a different time course for inhibiting DNA and RNA synthesis. Therefore, it is possible that the DNA analyses performed immediately after the 1 h exposure may significantly underquantitate the development of nuclear damage from compounds **47** and **104**. Protein synthesis was unaffected by any of the analogs' 1 h IC_{90}s in CHO cells at either time point (Figure 3c). This is similar to the pattern of macromolecular synthesis inhibition noted for the structurally similar drugs, the anthracyclines doxorubicin and daunorubicin, wherein DNA and RNA synthesis are significantly inhibited.[22]

The azonafide analogs, at their 1 h IC_{90} concentrations, each caused DNA SSB and DPC in the alkaline elution assays. Three compounds (**1**, **35** and **53**) also produced substantial DNA DSBs in the CHO cells. However, the efficiency of the different analogs varied considerably with analogs **47** and **104**, which have the higher cytotoxic potency, producing substantially less SSB, and essentially no DSB in the CHO cells. Conversely, analogs **1**, **35** and **53** produced DPCs in the CHO cells, whereas analogs **47** and **104** produced less. This represents a paradox wherein the more potent compounds distribute selectively into the nucleus, but produce less DNA damage than the other analogs when tested at equitoxic concentrations. This suggests that there may be different mechanisms and/or time course for cytotoxicity between the two groups of analogs.

Prior studies of anthracene drugs with structures similar to the azonafides have shown that alterations in the anthracene side chain can significantly alter both cytotoxic potency and DNA damaging efficiency. For example, Bowden *et al.* have observed differences in cytotoxicity and frequency of DNA SSB production in mouse L1210 leukemia cells between the anthracene-containing drugs bisantrene and mitoxantrone.[23] Therefore, our observations of altered cytotoxicity potency and DNA-damaging characteristics among the newer anthracene-based DNA intercalators is not unique.

When compared to amonafide, the azonafides produce similar types of DNA damage. Andersson *et al.*[9] have shown that amonafide produces SSB, DSB and DPC in the human myeloid leukemia cell line KBM-3. Although the types of lesions produced are conserved between the two types of compounds, the relative amounts of damage produced are not. For example, Andersson *et al.* reported a mean SSB/DPC ratio of about 1.32 in the KBM-3 cells. In the current CHO cell studies, the azonafides show an average SSB/DPC production ratio of 0.17 (ranging

from 0.11 to 0.22). This may relate to the different tumor cell lines used and/or that there are different mechanisms by which these DNA lesions are produced. Prior mechanistic studies with the azonafide series of compounds have shown that the strength of DNA intercalation, noted by resistance to thermal denaturation *in vitro*, roughly predicts the cytotoxic potency in murine L-1210 leukemia cells.[7] Thus, it is clear that the azonafides can bind non-covalently to DNA. However, as the current results with analogs **47** and **104** show, this binding may not always lead to the inhibition of DNA synthesis or Topo II-mediated strand breaks. Furthermore, the DNA damage produced by the azonafides is dependent on cellular interactions which do not involve direct DNA damage by the azonafides. Incubations of the drugs with SV40 DNA produced no alteration of DNA migration pattern after drug extraction (Figure 5), indicating that the drugs left the SV40 plasmid intact during the incubation period.

All of the analogs studied inhibited Topo II-mediated alteration of pRYG migration. However, there was no evidence of the trapping of Topo II–DNA cleavable complexes by these drugs. Lanes 5 and 6 show incubations of pRYG and Topo II with VP-16, a known Topo II inhibitor capable of trapping cleavable complexes.[22] In these lanes, increases in the form III and OC DNA bands are seen, indicating cleavable complex trapping. In similar incubations with MTX or the azonafide analogs, no increases in form III or OC DNA is seen. This observation suggests that the azonafide analogs studied may be catalytic inhibitors of Topo II as opposed to Topo II poisons such as VP-16.

Conclusion

Our findings indicate that the azonafides are potent cytotoxic agents whose mechanism of action may involve the ability to damage DNA as well as other, non-DNA-based possible mechanisms. The substantial differences in the extent of DNA damage produced among the analogs suggest variation in specific modes of action of each analog. The observations of macromolecular synthesis inhibition patterns and the production of protein-associated DNA strand breaks are consistent with the cellular consequences of Topo II inhibition. Although, based on the cell-free biochemical analyses data, it is clear that these drugs are capable of the inhibiting Topo II catalytic activity, but without producing the cleavable complex, which is thought to be the mechanism of DNA damage by other drugs of this type.

The azonafides thus represent a new group of antineoplastic agents that have shown activity against human and murine tumor cell lines, including multidrug-resistant sub-lines.[25] Additionally there appears to be a mechanism of action for these compounds that may be novel, as DNA damage production does not correlate with cytotoxic potency among a small group of analogs. Further study will be required to determine the exact mechanism of these drugs, which may lead to the ability to synthesize additional drugs of this type with increased antitumor activity.

Acknowledgments

The authors wish to thank James D Liddil for technical assistance in this study.

References

1. Braña MF, Castellano JM, Roldan CM, Vasquez D, Jiminez A. Synthesis and mode(s) of action of a new series of imide derivatives of 3-nitro-1,8-naphthoic acid. *Cancer Chemother Pharmacol* 1980; **4**: 61–6.
2. Braña MF, Sanz AM, Castellano JM, Roldan CM, Roldan C. Synthesis and cytostatic activity of benz(*de*)-isoquinolines-1,3-diones. Structure activity relationships. *Eur J Med Chem* 1981; **16**: 207–12.
3. Craig J, Crawford E. Phase II trial of amonafide in advanced prostate cancer: a Southwest Oncology Group study (meeting abstract). *Proc Am Soc Clin Oncol* 1989; **8**: 147.
4. Costanza ME, Berry D, Henderson IC. Amonafide: An active agent in the treatment of previously untreated breast cancer a Cancer and Leukemia Group B Study (CALGB 8624). *Clin Cancer Res* 1995; **1**: 699–704.
5. Saez R, Craig JB, Kuhn JG, *et al.* Phase I clinical investigation of amonafide. *J Clin Oncol* 1989; **7**: 1351–8.
6. Sami SM, Dorr RT, Alberts DS, Remers WA. 2-substituted 1,2-dihydro-3H-dibenz[*de*,*h*]isoquinoline-1,3-diones. A new class of antitumor agent. *J Med Chem* 1993; **36**: 765–70.
7. Sami SM, Dorr RT, Soloyam AM, Alberts DS, Remers WA. Amino-substituted 2-[2′-(dimethylamino)ethyl]-1,2-dihydro-3H-dibenz[*de*,*h*]isoquinoline-1,3-diones. Synthesis, antitumor activity, and quantitative structure–activity relationship. *J Med Chem* 1995; **38**: 983–93.
8. Dorr RT, Shipp NG, Lee KM. Comparison of cytotoxicity in heart cells and tumor cells exposed to DNA intercalating agents *in vitro*. *Anti-Cancer Drugs* 1991; **2**: 27–33.
9. Andersson BS, Beran M, Bakic M, Silberman LE, Newman RA, Zwelling LA. *In vitro* toxicity and DNA cleaving capacity of benzisoquinolinedine (nafidimide; NSC-308847) in human leukemia. *Cancer Res* 1987; **47**: 1040–4.

10. Remers WA, Dorr RT, Sami SM, Solyomas AS, Alberts DS. Quantitative structure–activity relationships of azonafide analogs. *Proc Am Ass Cancer Res* 1994; **35**: 337.
11. Alley MC, Scudiero DA, Monks A, Boyd MR. Feasibility of drug screening panels of human tumor cell lines using a microculture tetrazolium assay. *Cancer Res* 1988; **48**: 589–601.
12. Li LH, Timmins LG, Wallace TL, Krueger WC, Prairie MD, Im WB. Mechanism of action of didemnin B, a depsipeptide from the sea. *Cancer Lett* 1984; **23**: 279–288.
13. Ikegami S, Taguchi T, Ohashi M, Oguro M, Nagano H, Mano Y. Aphidicolin prevents mitotic cell division by interfering with the activity of DNA polymerase-alpha. *Nature* 1978; **275**: 458–60.
14. Young CW, Hodas S. Acute effects of cytotoxic compounds on incorporation of precursors into DNA, RNA and protein of HeLa monolayers. *Biochem Pharmacol* 1965; **14**: 205–14.
15. Kohn KW, Ewig RAG, Erickson LC, Zwelling LA. Measurement of strand breaks and cross-links by alkaline elution. In: Freidberg EC, Hanwalt PC, eds. *DNA repair: a laboratory manual of research procedures*. New York: Marcel Dekker; 1981; **1B**: 379–401.
16. Kohn KW, Ewig RAG. DNA–protein cross-linking by *trans*-platinum(II) diamminedichloride in mammalian cells, a new method of analysis. *Biochem Biophys Acta* 1979; **562**: 32–40.
17. Fornace AJ, Kohn KW. DNA–protein cross-linking by ultraviolet radiation in normal human and xeroderma pigmentosum fibroblasts. *Biochem Biophys Acta* 1976; **435**: 95–103.
18. Kohn KW, Grimek-Ewig RA. Alkaline elution analysis, a new approach to the study of DNA single-strand interruptions in cells. *Cancer Res* 1973; **33**: 1849–53.
19. Ross WE, Glaubiger D, Kohn KW. Qualitative and quantitative aspects of intercalator-induced DNA strand breaks. *Biochim Biophys Acta* 1979; **562**: 41–50.
20. Foglesong PD, Reckford C. Improved electrophoretic separation of supercoiled and relaxed DNA in the presence of ethidium bromide. *Biotechniques* 1992; **13**: 402–4.
21. Ludwig R, Alberts DA, Miller TP, Salmon SE. Evaluation of anticancer drug schedule dependency using an *in vitro* tumor clonogenic assay. *Cancer Chemother Pharmacol* 1984; **12**: 135–41.
22. Meriwether VD, Bachur NR. Inhibition of DNA and RNA metabolism by daunorubicin and Adriamycin in L1210 mouse leukemia. *Cancer Res* 1972; **32**: 1137–42.
23. Bowden GT, Roberts R, Alberts DA, Peng Y-M, Garcia D. Comparative molecular pharmacology in leukemic L1210 cells of the anthracene anticancer drugs mitoxantrone and bisantrene. *Cancer Res* 1985; **45**: 4915–20.
24. Ross W, Towe T, Glisson B, Yalowich J, Liu L. Role of topoisomerase II in mediating epipodophyllotoxin-induced DNA cleavage. *Cancer Res* 1984; **44**: 5857–60.
25. Dorr RT, Alberts DS, Sami SM, Remers WA. Consistent cytotoxic activity in multidrug resistant tumors for azonafide, a new anthracene analog of amonafide. *Proc Am Ass Cancer Res* 1991; **32**: 408.

(Received 10 December 1996; revised form accepted 3 January 1997)